*Youcef Bouhamidi[1], Ali Khelil[1*], Hadj Meliani Mohamed[2], Said Nechad[1], Larbi Loukarfi[1]*

# NUMERICAL INVESTIGATION OF THE GEOMETRY INFLUENCE ON THE AERODYNAMIC FIELDS OF THE FREE TURBULENT JETS

# NUMERIČKO ISTRAŽIVANJE UTICAJA GEOMETRIJE NA AERODINAMIČKA POLJA SLOBODNOG TURBULENTNOG MLAZA

Originalni naučni rad / Original scientific paper
UDK /UDC:

Rad primljen / Paper received: 14.11.2019

Adresa autora / Author's address:
1) Controls, Testing, Measurement and Simulation Mech. Laboratory, Hassiba Benbouali University of Chlef, Algeria
2) Lab. Theoret. Physics and Material Physics, LPTPM, Dep. of Mechanics, Faculty of Science, Hassiba Benbouali University of Chlef, Algeria email: hadjmeliani@univ-chlef.dz

**Keywords**
- swirling jet
- vane angle
- aerodynamic fields
- thermal homogenization
- thermal stability

**Ključne reči**
- vrtložno strujanje
- ugao lopatice
- aerodinamičko polje
- termička homogenizacija
- termička stabilnost

*Abstract*

*The objective of this study is to develop a numerical simulation of a flow from diffusers with different geometries. The main applications of this kind of diffuser are in forced ventilation and air conditioning. A detailed evaluation of the results face other numerical and experimental studies in the turbulent regime was examined for a turbulent jet in free mode. The k-ε turbulence model and RSM turbulence model are used in this investigation. Several flow parameters are tested such as the diffuser geometry, the number and angle of inclination of the swirled vane located in the diffuser associated with the concept of the swirl number. A comparison of numerical results with those available in literature is presented. Most of these comparisons are in good agreement with experimental data. By comparing changes in the axial and radial temperature, the configuration having an inclination vane of 60° and a diffuser having 14 vanes is a better temperature stability and large development in the radial direction with a significant decrease in the axial direction.*

*Izvod*

*Cilj prezentovanih istraživanja je razvoj numeričke simulacije strujanja u difuzorima različite geometrije. Osnovna primena ovakvih difuzora je kod veštačkog provetravanja i klimatizacije. Rezultati su detaljno obrađeni i upoređeni sa drugim numeričkim i eksperimentalnim studijama turbulentnog režima, u kojima je prisutno slobodno (daleko od zida) turbulentno strujanje. U istraživanju su upotrebljeni model k-ε turbulencije i RSM model turbulencije. Ispitivani su pojedini parametri strujanja, kao što su: geometrija difuzora, broj i ugao nagiba zakrivljenih lopatica u difuzoru, koji je povezan sa konceptom vrtložnog broja. Dato je poređenje dobijenih numeričkih rezultata sa rezultatima iz literature. Većina rezultata se dobro slaže sa eksperimentalnim podacima. Poređenjem aksijalne i radijalne temperaturske promene, konfiguracija sa nagibom lopatica 60° i difuzora sa 14 lopatica daje bolju temperatursku stabilnost, sa velikim povećanjem protoka u radijalnom pravcu u odnosu na veliko smanjenje u aksijalnom pravcu.*

## INTRODUCTION

The turbulent jets are among the most studied flows both because of their general availability in nature and their use in many industrial applications. The turbulent jets are an important practical interest in the technology of ventilation, cooling and drying /1-4/. The swirling jet is less known and very complex, it differs from the homogeneous turbulent jet by the existence of the tangential velocity component *W*. The application of the component of the tangential velocity (*W*) gives to the flow a component of rotation, shown by a dimensionless number (*S*) which is defined by the ratio of tangential flow on the axial flow:

$$S = G_\theta / RG_x = \int_{R_n}^{R_h} UWr^2 dr \Big/ \int_{R_n}^{R_h} R_n U^2 r dr \,, \qquad (1)$$

where: $G_\theta$ is the axial flux of tangential momentum; $G_x$ is the axial momentum flux; and $R$ is a characteristic radius; $R_n$ and $R_h$ are radii of centre body and inlet duct, in respect. Details of this equation are found in references /5-7/.

Studies show that the laws governing the real air movements are very complex, so the interest in the study of turbulent jets serves as a basic tool for understanding the phenomenon of air movements in free mode. The objective of the control of turbulent flow varies depending on the intended industrial application. We can control a turbulent flow to improve mixing using a diffuser with inclined vanes, but also to direct flow and change its orientation /8-10/. Turbulent diffusion leads to a very rapid environment homogenization. Swirling jets are particularly interesting in as much as they incorporate the characteristics of the rotary flow /11, 12/. The nature of the blowing system, the disposition, number of jets, the vanes inclination and temperature of the blown air are necessary parameters to achieve the swirling jet control, /13/.

Understanding the effects of turbulence, in particular the entrainment rate of the air and the stratification of the very high temperature lead to the efficiency of the air conditioning process. However, to our knowledge, the effects are barely studied, and therefore the effect of swirl diffuser geometry becomes interesting to study. Understanding the effects of the turbulence, in particular the air entrainment rate and the stratification of temperature lead to improvement of the efficiency of the air conditioning process. Felli et al. /14/ studied experimentally the dynamics of an impinging turbulent jet, generated by inclined vanes. They observed that the wall of the vanes changes the shape of the swirling jet causing it to spread outward and generate a recirculation zone around the vane support, wherein the swirling takes place before breakdown against the vane surface. The effect of different parameters on the development of the flow downstream of the vanes of a swirling jet generator in three dimensions has been widely studied, numerically by the standard $k$-$\varepsilon$ turbulence model, /15/. They obtained a good agreement with experimental results. Rajagopal, T.K.R., et al. /16/, numerically studied the devices to generate a both weak and strong swirling. They found that the diffuser with 8 vanes inclined with an angle of 45° produces a large recirculation zone. They noted that at low turbulence, the standard $k$-$\varepsilon$ turbulence model is sufficient, while for strong turbulence the RSM turbulence model is most appropriate. Ahmadvand et al. /17/ studied experimentally and numerically the influence of the inclination of the vanes on the heat transfer and on the flow increase of the turbulent fluid. These authors have confirmed that the use of the vanes leads to a higher heat transfer compared to those obtained from smooth tubes. Georges et al. /18/ conducted a systematic numerical study for single and multiple jet injection into a main flow by using the $k$-$\varepsilon$ standard turbulence model which is available in FLUENT code. Wang and Mujumdar /19/ have numerically investigated the flow and the mixing characteristics of multiple and multi-set three-dimensional confined turbulent round opposing jets in a novel in-line mixer using the standard $k$-$\varepsilon$ turbulence model. They had achieved a good agreement between the simulated and experimental results. Kucukgokoglanl et al. /20/ presented the performance of three different turbulence models for the prediction of turbulent flow of an oven with two burners against rotation. The numerical models used are the standard $k$-$\varepsilon$, and the RNG model. They noted that the standard $k$-$\varepsilon$ model and the RNG model are well established in the prediction of isothermal turbulence models of vortex flows, which have been successfully compared with experimental results. Yongson et al. /21/ analysed the air-conditioning system for a single room using CFD code. They studied several parameters such as temperature and velocity to determine the best position for the air-conditioning blower and also the area that is suitable for occupant comfort. According to their numerical results, the authors argue that the model RSM can have an independent solution of the mesh relative to the turbulence model $k$-$\varepsilon$ standard. Although the simulation using the RSM turbulence model takes more time compared to the $k$-$\varepsilon$ model, the independence of the mesh solution is more important.

## EXPERIMENTAL SETUP AND TECHNIQUES

The overview of the experimental setup considered herein is depicted in our previous papers. It is designed to investigate moderate and high Reynolds numbers (104 < $Re_0$ < 3.104). For more details regarding the setup and measuring techniques, the reader may consult references /10-12/. The swirl generator consists of: (a) cylindrical pipe of external diameter D = 56 mm; inside diameter d = 22 mm; and height H = 22 mm; (b) support of 14 vanes with height H = 22 mm; (c) vane thickness e = 1.7 mm and inclination = 60°, see Fig. 1.

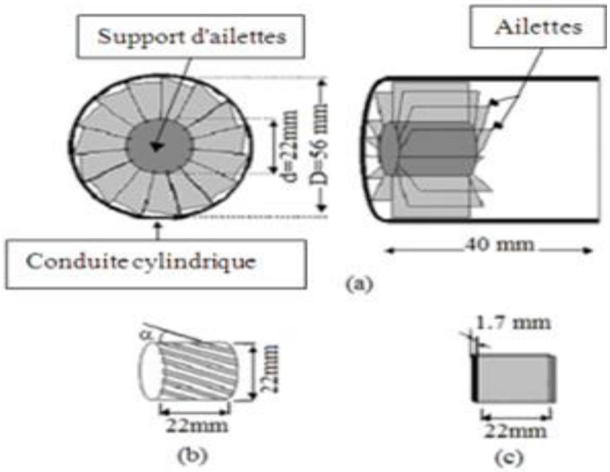


Figure 1. Scheme of swirl diffuser, /4/.

## NUMERICAL SIMULATION PROCEDURE

For a steady flow, a three-dimensional, incompressible and turbulent fluid having constant physical properties, the governing equations are the mass conservation equation and equations of momentum /22/, given as follows:

$$\frac{\partial U_i}{\partial x_i} = 0\,, \tag{2}$$

$$\rho \frac{\partial (U_i U_j)}{\partial x_j} = -\frac{\partial P}{\partial x_i} + \frac{\partial}{\partial x_j}\left[\mu\left(\frac{\partial U_i}{\partial x_j} + \frac{\partial U_j}{\partial x_i}\right) - \overline{\rho u_i u_i' u_j'}\right], \tag{3}$$

where: $U_i$ is the average velocity; $u_i'$ is the corresponding fluctuating component; $-\rho\overline{u_i' u_j'}$ are the Reynolds stresses that need to be modelled in order to ensure the closure of the equations. Note that here, the temperature variations are negligible, and the Mach number is low (< 0.3). Here, only the RSM model is used. It is now well known that in turbulent flows, where the effects of non-equilibrium are important, the hypothesis of Boussinesq is no longer valid, and the results of models based on this assumption may be inaccurate. Also, Reynolds stress models showed superior predictive performance relative to skilled isotropic models (based on such an assumption). Therefore, anisotropic models such as templates to Reynolds stresses (RSM) become necessary for a precise prediction of turbulent flow. In these models, the Reynolds stresses are governed by a transport equation that can be formulated as follows:

$$\underbrace{\frac{\partial}{\partial x_k}(\rho u_k \overline{u_i' u_j'})}_{\text{convection}} - \underbrace{\frac{\partial}{\partial x_k}\left(\mu \frac{\partial}{\partial x_k}\overline{u_i' u_j'}\right)}_{\text{molecular diffusion}} = \underbrace{D_{T,ij}}_{\text{turbulent dffusion}} + \underbrace{P_{ij}}_{\text{production}} + \underbrace{\phi_{ij}}_{\text{pressure strain}} + \underbrace{\varepsilon_{ij}}_{\text{dissipation}} + \underbrace{F_{ij}}_{\text{production by system rotation}},$$

where different terms (left to right) are, respectively: convection, diffusion, production, the stress-pressure, viscous dissipation and additional production constraints. Note that the terms of convection and production are correct, while the remaining terms are to be modelled /23/. For more details, the reader is referred to, i.e. references /24-26/.

## BOUNDARY CONDITIONS

The boundary conditions of the domain are imposed by nature within the limits considered (see Table 1): inlet or outlet of fluid, walls.

Table 1. Operating conditions, /4/.

| Fluid | air |
|---|---|
| Hydraulic diameter $D_{hydr}$ (m) | 0.047 |
| Inlet turbulence intensity (%) | 4 |
| Reynolds number (Re) | 30000 |
| Inlet temperature (K) | 363 |
| Inlet velocity (m/s) | 6 |
| Outlet pressure (atm) | 1 |

In addition, for each type of boundary condition, there are several conditional variants. Those of interest are described in the following paragraphs and illustrated in Fig. 2.

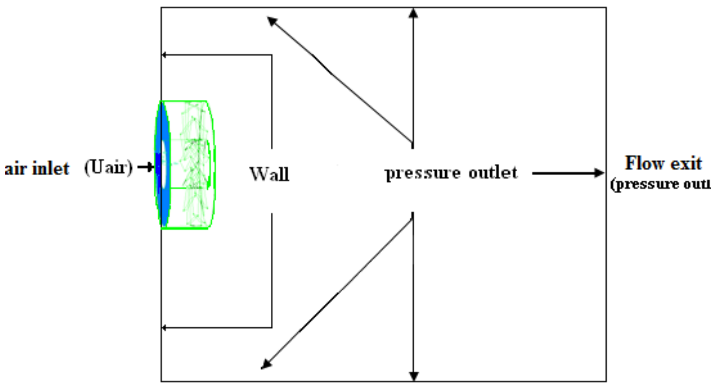


Figure 2. Computational domain and boundary.

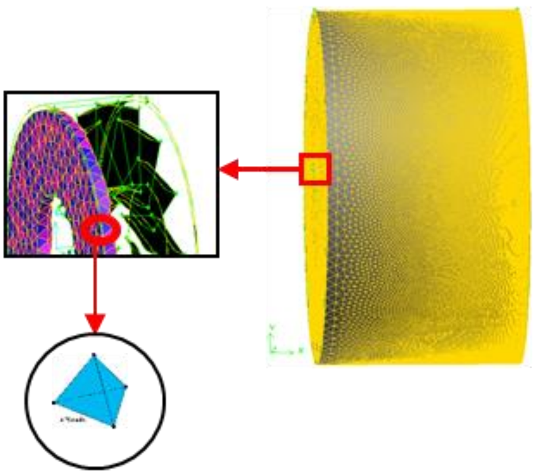

Figure 3. Grid sample in the inlet area.

## COMPUTATIONAL GRIDS CONSIDERED

The definition of the geometry and mesh are performed using the mesh generator 'GAMBIT' /8/, with the tetrahedral mesh form to four (04) nodes. A refinement of the areas in the vicinity of the diffuser exit is included to capture the different phenomena that can occur in these areas, including velocity and temperature gradients (Fig. 3). Calculations on different mesh are shown in Table 2. Figure 4 shows that the radial temperature solution does not change significantly. We can therefore conclude that the solution is independent of the mesh.

Table 2. Selection of different mesh and number of cells.

| Grid 1 | Grid 2 | Grid 3 | Grid 4 | Grid 5 |
|---|---|---|---|---|
| 760514 | 813171 | 1139252 | 1148961 | 1149927 |

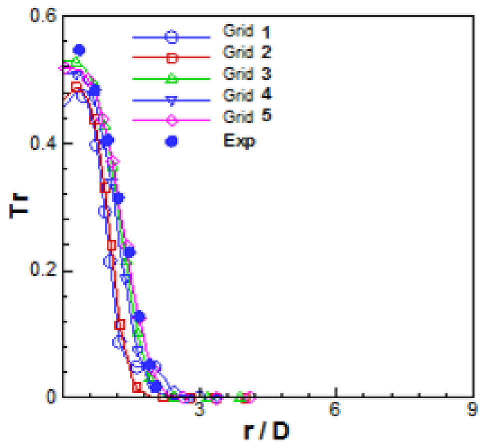


Figure 4. Solution independence of the mesh.

## RESULTS AND DISCUSSION

### *Determination of the optimal vanes number*

The axial dimensionless temperature profiles for different vane numbers (11, 14 and 17) predicted by the model RSM are presented in Fig. 5. Here, the dimensionless temperature $T_r$, $x$ and $y$ coordinates are normalized in the form $T_r = T - T_a$ / $T_0 - T_a$, $x/D$ and $y/D$, respectively, where $T$ is the jet temperature, $T_a$ is ambient temperature, and $T_0$ is maximum temperature of the air blowing at origin. The axial dimensionless temperature profile decreases from the origin, blowing along the centreline, to achieve further, ambient temperature. The maximum value of the axial temperature drops remarkably with the increase in the vanes number. On the other hand, far from the blowing origin (beyond $x/D = 8$) for the case of diffuser with 11 vanes number, the profile of dimensionless temperature significantly decreases in comparison with the other diffuser, with 14 and 17 vanes number, respectively. This figure shows that the diffuser with 17 vanes gives a maximum radial spreading, and the diffuser with 11 vanes gives rapid thermal stability. One can conclude that the diffuser with 14 vanes provides optimal radial jet spreading and thermal stability.

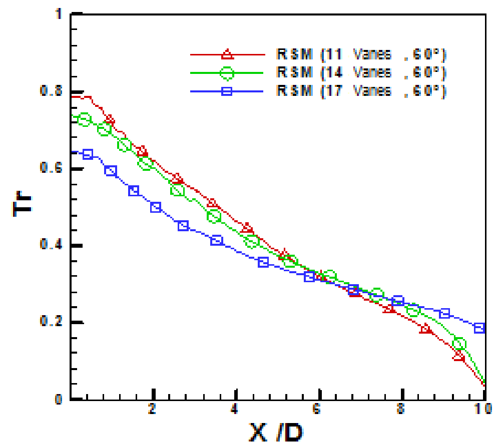


Figure 5. Axial dimensionless temperature profiles for different vanes numbers (11, 14 and 17) inclined by 60°, predicted by the model RSM.

Figure 6 shows that in the stations near to the blowing diffuser, the spreading in the radial direction is almost the same for vanes diffuser numbers 11, 14 and 17 respectively. In the stations far from the blowing diffuser, the number of vanes is important for the radial distribution of temperature. The radial temperature profile increases remarkably with increasing the number of vanes; thus, the development of the radial temperature is proportional to the number of vanes. We find that the number of vanes (14) has some very interesting results in relation to the number of vanes 11 and 17, or the radial development of the jet and thermal stabilization is satisfactory in the two diffuser configurations of 14 and 17 vanes.

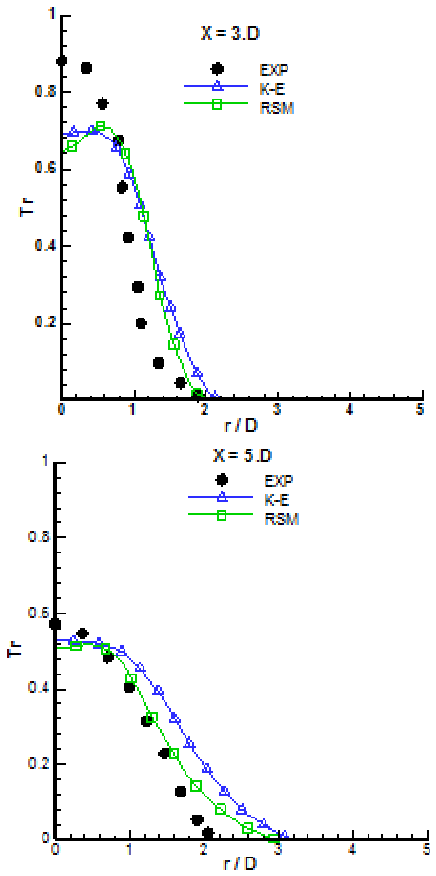


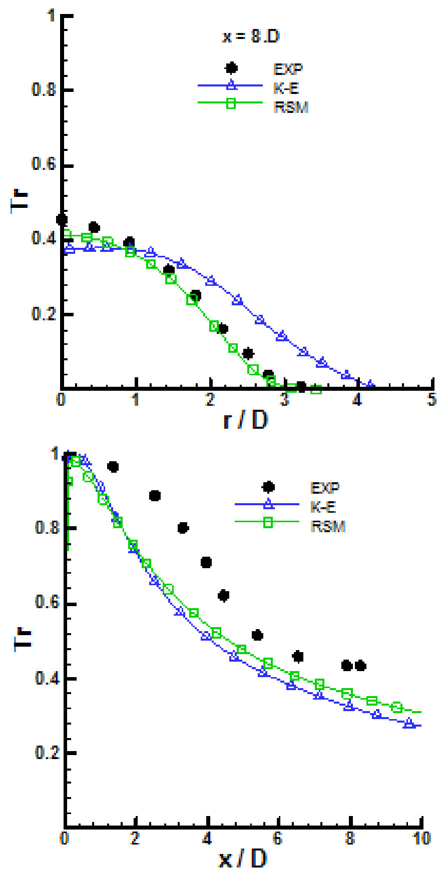


Figure 6. Radial and axial dimensionless temperature profiles for vane number 14, predicted by the *k*-$\varepsilon$ and RSM model in the axial stations *x/d* = 1, 3, 5, and 8.

Figure 6 presents a comparison between the present numerical results obtained using the calculation code 'Fluent' /9/ and experimental results /11, 12/. The results of experimental measurements and the adopted numerical model available are generally satisfactory as shown in Fig. 6 for the RSM model. Indeed, simplifying mathematical considerations are utilized to the operating commodities. So, for example, if we return to the basic assumptions used in the turbulence model *k*-$\varepsilon$, some clarifications are necessary for their impact on the calculation process. The numerical results show that the axial temperature predicted by the standard *k*-$\varepsilon$ turbulence model and the RSM are generally in good agreement with experimental data /11, 12/. Only the RSM model gives a fairly good agreement with the experimental results in the axial direction. The comparison of radial profiles of dimensionless axial velocity components, radial and tangential with experimental results measured at station $x/D = 5$ have been treated in Fig. 7. We noted that the *k*-$\varepsilon$ model underestimates the maximum value of velocity components in the radial station $r/d > 1$. Regarding the Reynolds stress model (RSM), it significantly improves the prediction of these values. As can be seen, the velocity profile predictions, dimensionless in the radial direction of using the Reynolds stress model are generally in good agreement with experimental data. Both models underestimate the magnitude of the velocity at the centreline, because of the internal recirculation area, as shown in Fig. 7. Outside this area, the standard $k$-$\varepsilon$ model and the Reynolds stress model, give a better overall agreement with experimental values, except for tangential velocities. We note that the numerical results are much more precise with the Reynolds stress model.

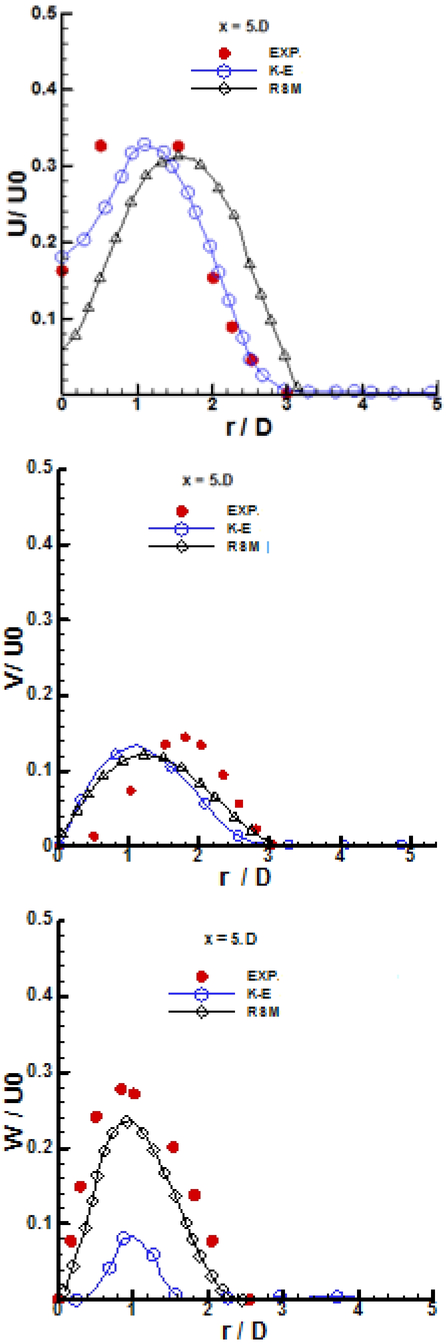


Figure 7. Radial distribution of components axial ($U$), radial ($V$) and tangential ($W$) velocity, by the standard $k$-$\varepsilon$ and RSM model, with experimental results at the station $x/D$ = 5.

## CONCLUSION

The optimization of parameters such as the geometry of the air blowing diffuser, the number of vanes, make it possible to improve the quality of thermal homogenization characterized by a large central recirculation zone inside this zone, the flow lines move radially to widen the average temperature distribution along the swirl jet axis. Maximum temperature is obtained at the level of the central recirculation zone which characterizes the mixing zone. The change in the radial temperature profile at a given distance from the blowing origin shows faster thermal stability of this temperature linked to a greater expansion of the jet. By comparing the evolution of the axial and radial temperature, the jet configuration with an inclination of 60° and a diffuser comprised of 11 vanes represents a better stability in radial temperature with a significant axial decrease. Of all the configurations studied, the latter quickly ensures maximum radial temperature stability. Overall, the results obtained with the Reynolds stress turbulence model (RSM) agree better with experimental data /11, 12/ compared to those obtained with the standard $k$-$\varepsilon$ turbulence model. The RSM model takes into account the effects of curvature of vanes and rapid changes in strain rate in a more rigorous manner than the standard $k$-$\varepsilon$ model.

## REFERENCES


1. Jawarneh, A.M., et al. (2017), *Double vortex generators for increasing the separation efficiency of the air separator*, Int. J Heat Technol. 35(3): 529-538. doi: 10.18280/ijht.350309
2. Sadeghiazad, M.B.M. (2017), *Experimental and numerical study on the effect of the convergence angle, injection pressure and injection number on thermal performance of straight vortex tube*, Int. J Heat Technol. 35(3): 651-656. doi: 10.18280/ijht.350324
3. Meghdir, A., Benabdallah, T., Dellil, A.Z.E. (2019), *Impact of geometry of electronic components on cooling improvement*, Int. J Heat Technol. 37(1): 167-178. doi: 10.18280/ijht.370121
4. Sadeghiazad, M.B.M. (2017), *Experimental study on thermal performance of Double Circuit Vortex Tube (DCVT) - Effect of heat transfer controller angle*, Int. J Heat Technol. 35(3): 668-672. doi: 10.18280/ijht.350327
5. Huang, Y., Yang, V. (2009), *Dynamics and stability of lean-premixed swirl-stabilized combustion*, Prog. Energy Combust. Sci. 35(4): 293-364. doi: 10.1016/j.pecs.2009.01.002
6. Lalmi, D., Hadef, R. (2017), *Numerical study of the swirl direction effect at the turbulent diffusion flame characteristics*, 35(3): 520-528. doi: 10.18280/ijht.350308
7. Mansouri, Z., Aouissi, M., Boushaki, T. (2016), *A numerical study of swirl effects on the flow and flame dynamics in a lean premixed combustor*, Int. J Heat Technol. 34(2): 227-235. doi: 10.18280/ijht.340211
8. Pratte, B.D., Keffer, J.F. (1972), *The swirling turbulent jet*, ASME J Basic Eng. 94(4): 739-748. doi: 10.1115/1.3425538
9. Davis, M.R. (1982), *Variable control of jet decay*, AIAAJ, 20 (5): 606-609. doi: 10.2514/3.7934
10. Roudane, M., Loukarfi, L., Khelil, A., Hemis, M. (2013), *Numerical investigation of thermal characteristics of confined rotating multi-jet*, Mech. & Industry, 14(4): 317-324. doi: 10.1 051/meca/2013071
11. Khelil, A., Naji, H., Braikia, M., Loukarfi, L. (2015), *Comparative investigation on heated swirling jets using experimental and numerical computations*, Heat Trans. Eng. 36(1): 43-57. doi: 10.1080/01457632.2014.906279
12. Braikia, M., Loukarfi, L., Khelil, A., Naji, H. (2012), *Improvement of thermal homogenization using multiple swirling jets*, Therm. Sci. 16(1): 239-250. doi: 10.2298/TSCI101026131B
13. Branci, N. (2009), Caractéristiques d'un multi jet tourbillonnaire à orifices déséquilibrés en position et en température, Thèse d'ingénieur en mécanique, Département Mécanique, Faculté de technologie, Université Hassiba Benbouali de Chlef, Algérie.

(in French, 'Characteristics of a swirling multi-jet with vanes unbalanced in position and temperature', Master Thesis in Mech. Eng.)
14. Felli, M., Falchi, M., Pereira, F.J.A. (2010), *Distance effect on the behavior of an impinging swirling jet by PIV and flow visualizations*, Exp. Fluids, 48(2): 197-209. doi: 10.1007/s00348-009-0723-5
15. Wang, S.J., Mujumdar, A.S. (2007), *Flow and mixing characteristics of multiple and multi-set opposing jets*, Chem. Eng. Process.: Process Itensif. 46: 703-712. doi: 10.1016/j.cep.2006.09.006
16. Rajagopal, T.K.R., Ganesan, V. (2008), *Study on the effect of various parameters on flow development behind vane swirlers*, Int. J Ther. Sci. 47(9): 1204-1225. doi: 10.1016/j.ijthermalsci.2007.10.019
17. Ahmadvand, M., Najafi, A.F., Shahidinejad, S. (2010), *An experimental study and CFD analysis towards heat transfer and fluid flow characteristic of decaying swirl pipe flow generated by axial vanes*, Meccanica, 45: 111-129. doi: 10.1007/s11012-009-9228-9
18. Giorges, A.T.G., Forney, L.J., Wang, X. (2001), *Numerical study of multi-jet mixing*, Chem. Eng. Res. Des. 79(5): 515-522. doi: 10.1205/02638760152424280
19. Wang, S.J., Mujumdar, A.S. (2007), *Flow and mixing characteristics of multiple and multi-set opposing jets*, Chem. Eng. Proc.: Process Itensif. 46(8): 703-712. doi: 10.1016/j.cep.2006.09.006
20. Kucukgokoglan, S., Aroussi, A., Pickering, S.J. (2002), *CFD simulations of two co-rotating burner flows*, in Proc. 6th Asian Symp. on Visualization, 176: 1-6.
21. Yongson, O., Badruddin, I.A., Zainal, Z.A., Aswatha Narayana, P.A. (2007), *Airflow analysis in an air conditioning room*, Build. Environ. 42(3): 1531-1537. doi: 10.1016/j.buildenv.2006.01.002
22. El Drainy, Y.A., Saqr, K.M., Aly, H.S., Mohd Jaafar, M.N. (2009), *CFD Analysis of incompressible turbulent swirling flow through Zanker plate*, Eng. Appl. Comp. Fluid Mech. 3(4): 562-572. doi: 10.1080/19942060.2009.11015291
23. Fluent 6.3, User's Guide, Fluent Inc., Lebanon, NH, USA, 2009.
24. Nemdili, F., Azzi, A., Theodoridis, G., Jubran, B.A. (2008), *Reynolds stress transport modeling of film cooling at the leading edge of a symmetrical turbine blade model*, Heat Trans. Eng. 29(11): 950-960. doi: 10.1080/01457630802186064
25. Gambit (2002), A CFD preprocessor, Gambit 2.0 User's Guide, Vol.2, Canterra, Lebanon, NH, USA.
26. Chaware, P., Sewatkar, C.M. (2017), *Effects of tangential and radial velocity on the heat transfer for flow through pipe with twisted tape insert-turbulent flow*, Int. J Heat Technol. 35(4): 811-820. doi: 10.18280/ijht.350417

## NOMENCLATURE

| | |
|---|---|
| $G_\theta$ | axial flux of tangential momentum |
| $G_x$ | axial momentum flux |
| $r$ | radial coordinate of air flow (m) |
| $R$ | characteristic radius (m) |
| $R_h$ | radius of the inlet duct (m) |
| $R_n$ | radius of the centre body (m) |
| $S$ | swirl number (dimensionless) |
| $T$ | temperature of jet (K) |
| $T_a$ | ambient temperature (K) |
| $T_0$ | maximum temperature of the air blowing at origin |
| $T_r$ | dimensionless temperature (= $(T - T_a)/(T_0 - T_a)$) |
| $U$ | mean axial velocity based on flow rate (m/s) |
| $W$ | mean tangential velocity (m/s) |
| $x$ | axial coordinate of the air flow (m) |
| $u'$ | fluctuating velocity (m/s) |
| $-\rho\overline{u_i'u_j'}$ | Reynolds stresses (kg/ms$^2$) |